

RNF180 Suppresses Methylation of ADAMTS9 DNA Promotor by Ubiquitinating DNMT3A Inhibiting Metastasis in Gastric Cancer

Weilin Sun

Tianjin tumor hospital

Jingyu Deng (✉ dengery@126.com)

Tianjin Tumor Hospital

Gang Ma

Tianjin Tumor Hospital

Li Zhang

Tianjin Tumor Hospital

Pengliang Wang

Tianjin Tumor Hospital

Huifang Liu

Tianjin tumor hospital

Nannan Zhang

Tianjin Tumor Hospital

Zizhen Wu

Tianjin Tumor Hospital

Yinping Dong

Tianjin tumor hospital

Fenglin Cai

Tianjin Tumor Hospital

Liqiao Chen

Tianjin Tumor Hospital

Zhenzhen Zhao

Tianjin tumor hospital

Han Liang

Tianjin tumor hospital

Research

Keywords: ADAMTS9, ring finger protein 180, gastric cancer, metastasis

Posted Date: May 29th, 2020

DOI: <https://doi.org/10.21203/rs.3.rs-30779/v1>

License:   This work is licensed under a Creative Commons Attribution 4.0 International License.

[Read Full License](#)

Abstract

BACKGROUND: A disintegrin-like and metalloprotease with thrombospondin type 1 motif 9 (ADAMTS9) is hypermethylated and inhibits the proliferation of various cancers. In this study, we demonstrated that the expression of ADAMTS9 was associated with the lymphatic metastasis of gastric cancer (GC) and elucidated the down- and upstream molecular pathways in GC progression.

METHODS: The study explored the expression level, biological function, clinical application, and involved molecular mechanism of ADAMTS9 in GC.

RESULTS: In 135 GC tissue samples, ADAMTS9 expression level was significantly correlated with the pN stage, the number of metastatic lymph nodes (LNs), and the overall survival of patients with GC. The *in vitro* and *in vivo* experiments showed that ADAMTS9 attenuated the viability and motile capacity of GC cells. Mechanistic investigations revealed that ADAMTS9 significantly inhibited the transcription of C–C motif chemokine ligand 5 (CCL5)/C–X–C motif chemokine ligand 11 (CXCL11). This effect impaired the migration and invasion in GC cells. This study revealed that the hypermethylation level in the promotor of ADAMTS9 gene was mainly mediated by DNA-methyltransferase(DNMT) 3A, which reduces ADAMTS9 expression in GC. Ring finger protein (RNF) 180 could promote DNMT3Aubiquitination and degradation, thereby restoring the ADAMTS9 expression in GC cells.

CONCLUSIONS: ADAMTS9 expression is restored by the RNF180 via suppressing the promotor methylation of the ADAMTS9 gene. ADAMTS9 inhibits metastasis and improves the prognosis of patients with GC via CCL5/CXCL11-dependent pathway. Thus, ADAMTS9 should be considered as a predictor of LN metastasis and a therapeutic target in GC.

Background

Gastric cancer (GC) is currently the 5th most common malignant tumor and the 3rd leading cause of cancer-related death¹. GC shows a strong tendency to spread locally and metastasize via the lymph nodes (LN) because of the abundant blood and lymphatic vessels in the gastric area. Although surgery has significantly improved the prognosis of patients, the wide extent of LN metastasis always limits the management and treatment of patients with GC, thereby leading to a poor 5-year survival rate of 20%–30% in patients with advanced GC². Thus, tracking and identifying a novel effective biomarker that contributes to metastasis remains imperative for GC.

A disintegrin-like and metalloproteinase with thrombospondin motifs (ADAMTS) is a family of secreted, multi-domain matrix-associated zinc metalloendopeptidases with 19 members³. ADAMTS family proteins are originally identified as the cleave-type substrates in the extracellular matrix. These proteins participate in numerous physiological processes and diseases, such as cardiovascular disease⁴, arthritis⁵, cancer⁶, and angiogenesis⁷. ADAMTS9 is a member of the ADAMTS family that acts as a tumor suppressor in several types of human cancers, such as esophageal⁸, nasopharyngeal⁹, breast¹⁰ and colorectal

cancers¹¹, and GC¹². However, the correlation between ADAMTS9 and LN metastases in GC has been rarely reported, and the downstream molecular pathway remains unclear.

The promotor methylation of tumor-suppressor genes or tumor-related genes is usually involved in the multistep progression of tumor carcinogenesis and the development of cancer¹³. The hypermethylation of the promotor of ADAMTS9 gene is the most important cause that decreases or silences the expression of ADAMTS9¹². The mechanism of modulating the promotor methylation of ADAMTS9 gene remains unclear. The novel E3 ubiquitin ligase involved in protein ubiquitination process, ring finger protein (RNF) 180 is a tumor suppressor in GC¹⁴. Ubiquitination plays an essential role in protein post-translation modification and is involved in various processes of tumorigenesis and tumor development¹⁵. Identifying the substrate of E3 ubiquitin ligase and improving the understanding of the ubiquitination process benefit clinicians in tumor treatment. Through the correlation analysis from the GEPIA database (<http://gepia.cancer-pku.cn/>), we found that the mRNA expression level of RNF180 might have a positive correlation with ADAMTS9. In addition, the immunohistochemistry (IHC) staining of tissue microarrays (TMAs) with 135 GC tissue samples also showed a significant positive correlation between RNF180 and ADAMTS9 expression. Thus, we hypothesized that RNF180 may suppress the methylation of ADAMTS9 DNA promotor to restore the ADAMTS9 expression in GC. In this study, we initially explored the interactional substrate of RNF180 and revealed the potential molecular mechanism of mediating ADAMTS9 expression in GC.

In present study, we demonstrated that the low expression of ADAMTS9 was closely associated with advanced pN stage and poor survival outcome in GC. ADAMTS9 attenuated the viability and motile capacity of GC cells. We uncovered that ADAMTS9 was partly located in the cell nucleus region and inhibited the transcription of chemokine ligand 5 (CCL5) and C-X-C motif chemokine ligand 11 (CXCL11). This effect impaired the migration and invasion behavior of GC. ADAMTS9 expression was mainly regulated by the promotor methylation level via modifying the expressions of DNA-methyltransferase (DNMT)3A. RNF180 promotes DNMT3A ubiquitination and degradation, thereby restoring the expression of ADAMTS9 in GC. Thus, our study identified ADAMTS9 as the potential target for the prediction of LN metastasis and prognosis and elucidated the potential up- and downstream molecular pathways in GC.

Methods:

Patients and tissue samples

After curative gastrectomy, 135 pairs of GC tissues and matched adjacent non-tumor tissues were retrieved from the Department of Gastroenterology, Tianjin Medical University Cancer Institute and Hospital (Tianjin, China) between August 2004 and December 2007. These matched tissues were then sent to Shanghai Outdo Biotech Company (Shanghai China) for TMAs (Cat No. T14-501 TMA1-3). Tissue total RNA was extracted from 16 pairs of randomly selected GC tissue and matched adjacent non-tumor tissues after gastrectomy between July 2018 and December 2018. All tumor and adjacent non-tumor tissue samples were histologically verified. The patients in this study were not subjected to radiation, chemical, or

biological treatment before potential curative gastrectomy. Adjuvant chemotherapy or radiotherapy was not routinely administered to the patients. The clinicopathological characteristics of the two cohorts are summarized in **Table 1** and **Supplementary Table S1**, respectively. Patient consent was obtained for the use of the tissue samples. The study protocol and permission for the use of the clinical data were given by the Institutional Research Ethics Committee of Tianjin Medical University Cancer Institute and Hospital (Tianjin, China).

Table 1
Clinicopathologic Features of ADAMTS9 Expression in Gastric Cancer Tissues

Characteristics	ADAMTS9		c ² value	P value
	High expression	Low expression		
Gender				
Male	45	45	0.018	0.894
Female	19	20		
Age				
<60	33	37	0.373	0.541
≥60	31	28		
Tumor location				
Upper third	13	10	1.830	0.608
Middle third	8	5		
Lower third	29	36		
More than 2/3 stomach	14	14		
Tumor size				
<5cm	25	27	0.082	0.774
≥5cm	39	38		
pT stage				
pT2	5	4	0.326	0.850
pT3	4	3		
pT4	55	58		
pN stge				
pN0	18	10	10.043	0.018*
pN1	9	4		
pN2	15	11		
pN3	22	40		
pTNM stage				

Note: 1, some data has lost; a, continuity correction test; b, fisher exact test; *, P<0.05;

I	3	1	2.480	0.285 ^b
II	18	13		
III	43	51		
Lauren type				
Intestinal	13	12	3.066	0.216
Diffuse	46	52		
Mixed	5	1		
Borrmann type¹				
□	0	1	3.271	0.352
□	9	14		
□	33	25		
□	5	6		
Note: 1, some data has lost; a, continuity correction test; b, fisher exact test; *, P<0.05;				

Follow-up

After curative surgery, follow-up was performed for all patients every 3–6 months for 2 years, after which follow-up was performed every year, until death, or until deadline. The median follow-up for the entire cohort was 34.0 months (range: 2–75). The follow-up of all patients who were included in this study was completed in September 2012. B ultrasonography, CT scans, chest X-ray, and endoscopy were obtained with every visit.

IHC

IHC was performed on the TMAs of resected specimens. The 1.5 mm-diameter tissue cores from randomly selected GC tissues and matched adjacent non-tumor tissues were used for TMA preparation. The antibodies are as shown in **Supplementary Table S2**. The staining intensities (0, negative; 1+, weak; 2+, moderate; and 3+, strong) were recorded. The percentage of immunostaining and the cytoplasmic expression were assessed by H-score system. The formula for the H-score is: $\text{histoscore} = \sum (I \times P_i)$, where I = intensity of staining and P_i = percentage of stained tumor cells, producing a cytoplasmic score ranging from 0 to 300.

Cycloheximide (CHX) pulse-chase assay and MG132 assay

To detect the half-life of DNMT3A, we treated the stable transfected AGS and BGC-823 cells with CHX (100 mg/mL) for the indicated times. MG132 assay was performed to determine the degradation via proteasome. AGS and BGC-823 cells were incubated with proteasome inhibitor MG132 (10 μ M) for 12 h. Western blot analysis was then performed to detect DNMT3A expressions.

Co-immunoprecipitation assay

HEK293T cells were seeded into 6-well plates and transiently transfected with empty vector, pCMV-RNF180-myc plasmid, or pCMV-DNMT3A-flag plasmid. After transfection for 36 h, cells were treated with 10 mM MG132 for 12 h. Total proteins were then extracted using Nonidet P-40 lysis buffer supplemented with PSMF (#8553, cst). Immunoprecipitation Kit-DYKDDDDK (Flag®) Tag Immunomagnetic Beads (TB101274, Sino Biological, North Wales, PA, USA) and Immunoprecipitation Kit -MYC Tag Immunomagnetic Beads (TB100029, Sino Biological, North Wales, PA, USA) were adopted for collecting the immunoprecipitated proteins. The immunoprecipitated proteins were measured by the Western blot analysis.

Ubiquitination assay

To evaluate the ubiquitination of DNMT3A, we transiently transfected empty vector, pCMV-DNMT3A-flag plasmid, pCMV-RNF180-myc plasmid or pCMV-HA-UB plasmid the HEK293T cells. After transfection for 36 h, HEK293T cells were incubated with MG132 (10 μ M) for 12 h. The correlated proteins were extracted and analyzed by the co-immunoprecipitation assay.

Genome-wide mRNA sequencing analysis

BGC-823 cells were stably transfected with pCNA3.1-ADAMTS9 vector or pCNA3.1 empty vector. Total RNA was then extracted using the mirVana miRNA Isolation Kit (Ambion, Foster City, CA, USA) according to the manufacturer's protocol. RNA integrity was evaluated using the Agilent 2100 Bioanalyzer (Agilent Technologies, Santa Clara, CA, USA). The samples with RNA integrity number ≥ 7 were subjected to subsequent analysis. The libraries were constructed using TruSeq Stranded mRNA LTSample Prep Kit (Illumina, San Diego, CA, USA) according to the manufacturer's instructions. P value < 0.05 and foldchange > 1.50 or < 0.67 were set as the threshold for significantly different expression. The hierarchical cluster analysis of differentially expressed genes (DEGs) was performed to explore gene expression patterns. The GO enrichment and KEGG pathway enrichment analysis of DEGs were performed using the R software¹⁶. Transcriptome sequencing and analysis were conducted by OE Biotech Co., Ltd. (Shanghai, China).

MassARRAY analysis of the methylation level of ADAMTS9

Total DNA were extracted using the DNA sample Kit (TIANGEN Biotech, Beijing, China) following the manufacturer's protocol. The quantitative DNA methylation analysis of ADAMTS9 was then performed using the MassARRAY platform (Agena; BioMiao Biological Technology, Beijing, China). The MassARRAY Compact MALDI-TOF (Agena; BioMiao Biological Technology, Beijing, China) was used to collect the mass spectra, and the EpiTYPER software (Agena; San Diego, CA) was used to calculate the methylation ratio.

Other methods and statistical analysis are available in the **Supplementary dataset**.

Results

ADAMTS9 was associated with LN metastases and survival outcome in patients with GC

We examined the mRNA levels of ADAMTS9 in the 16 pairs of tumor and adjacent non-tumor tissues. A total of 9/16 of tumor tissues showed lower mRNA expression level compared with that of adjacent non-tumor tissues (**Figure 1A**), which were classified into low expression group. The correlation between the clinicopathological characteristics and mRNA expression of ADAMTS9 was analyzed. ADAMTS9 mRNA expression was significantly associated with pN stage ($P=0.044$) and Lauren type ($P=0.019$) (**Supplementary Table S1**). Patients with low ADAMTS9 mRNA expression were at high risk with increased metastatic LNs (12.89 ± 3.49 vs 2.571 ± 1.020 , $P=0.024$, **Figure 1B**).

We further examined the protein expression of ADAMTS9 in GC tissues. With the IHC staining, ADAMTS9 protein expression was found in the cytoplasm and nucleus of the gastric tissue cells (**Figures 1C and 3A**). H-score was used to evaluate the ADAMTS9 protein expression. A total of 111 pairs of GC tissues and adjacent non-tumor tissues and additional 18 GC tissues were completely saved and well stained. Compared with that of adjacent non-tumor tissue, the H-Score of GC tissues was significantly decreased ($P=0.008$, **Figure 1D**). Exactly 129 GC tissues were then divided into the low and high expression groups according to the median of H-score as the cut-off value. The clinicopathological characteristics are shown in **Table 1**. Univariate analysis suggested that patients with low ADAMTS9 expression was associated with advanced pN stage ($P=0.018$). We further examined the number of LNs involvement between the two groups, and the number of metastatic LNs of high expression group was significantly decreased (11.38 ± 11.64 vs 6.73 ± 7.63 , $P=0.007$; **Figure 1E**). ADAMTS9 expression was closely correlated to the LN metastasis.

To evaluate the prognostic value of ADAMTS9 expression in GC, we employed the Kaplan–Meier analysis. **Figure 1F** shows that patients with GC with low ADAMTS9 expression had a significantly poorer 5-year survival rate than those with high expression ($P=0.007$). To remove the various interference factors, we also acquired the multivariate Cox regression analysis. In multivariate Cox regression analysis, ADAMTS9 expression level (HR 1.602, 95%CI 1.069–2.399, $P=0.022$) was an independent predictor of the prognosis of patients with GC with the lowest Akaike information criterion (AIC, AIC=71.555) and Bayesian information criterion (BIC, BIC=88.714, **Table 2**). We demonstrated the crucial effect on the survival

outcomes through stratification by pN stage. In the subgroup of patients with pN3 stage, ADAMTS9 expression was significantly associated with survival outcomes (P=0.011, **Figure 1F**).

Table 2

Univariate and multivariate Cox proportional Hazard models for overall survival of gastric cancer patients

Predictor	Univariate Analysis		Multivariate Analysis		AIC	BIC
	HR(95% CI)	P	HR (95% CI)	P		
Gender						
Female vs male	1.372(0.905-2.079)	0.136				
Age						
≥60 vs <60	1.514(1.012-2.245)	0.039*	1.528(1.005-2.323)	0.047*	74.730	91.889
Tumor size						
≥5cm vs <5cm	1.888(1.250-2.851)	0.003**	1.591(1.041-2.430)	0.032*	72.686	89.844
Tumor location						
Middle 1/3 vs up 1/3	1.232(0.588-2.584)	0.580				
Low 1/3 vs up 1/3	0.948(0.545-1.649)	0.851				
>2/3 stomach vs up 1/3	1.235(0.661-2.307)	0.508				
Lauren type						
Diffuse vs intestinal	1.144(0.677-1.934)	0.615				
Mixed vs intestinal	1.621(0.637-4.123)	0.311				
Borrmann type						
II vs I	0.552(0.073-4.173)	0.565				
III vs I	0.385(0.052-2.847)	0.350				
IV vs I	0.512(0.064-4.113)	0.529				
pT stage						

Note: AIC, Akaike information criterion; BIC, Bayesian information criterion;
 *, P<0.05; **, P<0.01; ***, P<0.001.

pT3 vs pT2	0.547(0.164-1.821)	0.326				
pT4 vs pT2	0.788(0.381-1.628)	0.519				
pN stage						
pN1c vs pN0	0.958(0.397-2.315)	0.925	0.784(0.319-1.929)	0.597	81.240	92.680
pN2 vs pN0	1.745(0.911-3.341)	0.093	1.480(0.758-2.889)	0.251		
pN3 vs pN0	2.828(1.638-4.883)	<0.001***	2.231(1.273-3.912)	0.005**		
Expression of ADAMTS9						
Low vs high	1.732(1.166-2.573)	0.009**	1.602(1.069-2.399)	0.022*	71.555	88.714
Note:AIC, Akaike information criterion; BIC, Bayesian information criterion; *,P<0.05; **, P<0.01;***, P<0.001.						

Low-expression of ADAMTS9 in GC cell lines

The ADAMTS9 mRNA expression in 10 types of human GC cell lines and normal GES-1 was determined. Excluding SNU-1 and HGC-27, the mRNA expression of ADAMTS9 in 8/10 GC cell lines was lower than that in GES-1 (**Figure 2A**). To confirm whether the protein expression follows its mRNA expression, we tested seven GC cell lines and GES-1. Western blot analysis results showed that ADAMTS9 protein was silenced or down-regulated in 6/7 GC cell lines (**Figure 2B**), which was consistent with their mRNA expression. The low ADAMTS9 expression in most GC cell lines might be a tumor suppressor.

ADAMTS9 suppressed GC cell proliferation and viability

To explore the biological function of ADAMTS9 in GC cells, we overexpressed ADAMTS9 in AGS, BGC-823, and SGC-7901 cells through the pCND3.1-ADAMTS9 plasmid. The mRNA and protein expression of ADAMTS9 were proven by RT-PCR and Western blot analysis (**Figure 2c** and **Supplementary Figure S1A**). CCK8 assay and cell growth curve results then showed that ADAMTS9 suppressed cell proliferation and viability (**Figure 2D** and **Supplementary Figure S1B**). The results of colony formation assays were consistent with the CCK8 assay results (**Figure 2E** and **Supplementary Figure S1C**). Thus, ADAMTS9 inhibited GC cell proliferation and viability.

ADAMTS9 inhibited tumor growth in nude mouse

We investigated the effects of ADAMTS9 *in vivo*. The size of subcutaneous tumor transfected with ADAMTS9 was significantly decreased than that in tumor transfected with empty vector. The growth curve and tumor weight figure of the subcutaneous tumor are shown in **Figure 2F**. ADAMTS9 inhibited tumor growth *in vivo*.

ADAMTS9 inhibited GC cells migration and invasion

The effects of ADAMTS9 expression on AGS, BGC823, and SGC-7901 cells on migration and invasion were also assessed. Wound healing assay result showed that the migration distances of over-expressed ADAMTS9 group were significantly reduced compared with that of the control group (AGS, 48H, $P<0.001$; BGC-823, 48H, $P=0.009$; and SGC-7901 36H $P<0.001$, **Figure 2G** and **Supplementary Figure S1D**). To confirm the effect on migration and invasion, we further examined motile ability by using Transwell chambers. Similar results were obtained, thereby indicating that the number of migratory and invaded AGS and BGC-823 cells was significantly decreased in the over-expressed ADAMTS9 group (AGS, BGC-823, and SGC-7901; migration: $P=0.003$, $P=0.010$, and $P=0.010$; invasion: $P=0.035$, $P=0.010$, and $P=0.004$; **Figure 2H** and **Supplementary Figure S1E**). ADAMTS9 inhibited GC cell migration and invasion.

ADAMTS9 inhibited GC metastasis through CCL5 and CXCL11 pathways

With IHC results for ADAMTS9, we found ADAMTS9 was partly located in the nucleus of the gastric tissue cells (**Figure 3A**). To elucidate the downstream molecular mechanism of ADAMTS9, we performed the mRNA sequencing analysis of BGC-823 cells transfected with pCDNA3.1-ADAMTS9 plasmid or pCDNA3.1 empty plasmid. Among the 20031 genes screened by the mRNA sequencing, 183 genes showed significant decrease or increase greater than 1.5-fold change (**Figure 3B**). Several DEGs were significantly up- or down-regulated in AGS and BGC-823 cells by real-time PCR analysis (**Figure 3F**). The gene information and potential biological functions of these DEGs are shown in the **Figure 3D** and **Figure 3E**. To further examine the key roles of ADAMTS9 on GC metastasis, we performed the KEGG pathway analysis (**Figure 3C**). The chemokine signaling pathway and the cytokine-cytokine receptor interaction pathway were included in the top 20 enrichment pathways (**Supplementary Figure S2**). Two of the significantly down-regulated genes, namely, CCL5 and CXCL11, played a crucial role in metastasis. To further validate this finding, we detected the down-regulated mRNA and protein expression of CCL5 and CXCL11 in the four GC cell lines (AGS, BGC-823, SGC-7901, and NCI-N87; **Figures 3G** and **3H**). The relationships between ADAMTS9 and CCL5 and between ADAMTS9 and CXCL11 in human GC tissues were further explored. We performed immunohistochemical staining to examine the correlation between the protein levels of CCL5, CXCL11, and ADAMTS9 in the GC tissue specimens on TMAs (**Supplementary Figure S3**). **Figure 3I** shows that the protein expressions of CCL5 and CXCL11 were both negatively associated with ADAMTS9 protein expression (CCL5, $N=122$, Pearson $r=-0.308$, $P=0.001$; CXCL11, $N=125$, Pearson $r=-0.501$, $P<0.001$). ADAMTS9 inhibited the GC cell metastasis by down-regulating CCL5 and CXCL11 expressions.

DNMT3A mainly regulated the promotor methylation of ADAMTS9 gene

According to the MethHC database(<http://methhc.mbc.nctu.edu.tw/php>), the ADAMTS9 promotor is hypermethylated in the GC, thereby leading to the down-regulation or silencing of the expression of ADAMTS9 (**Figure 4A**). We also validated the hypermethylation of ADAMTS9 promotor by using the 5-Aza (2 μ M) treatment in the AGS and BGC-823 cell lines. **Figure 4B** shows that the mRNA expression of ADAMTS9 significantly increased after 5-Aza (2 μ M) treatment. MassARRAY analysis was adopted to examine the methylation of ADAMTS9 DNA promotor. **Figure 4C** and **Supplementary Figure S4A** show that aberrant methylation was detected in BGC823 cells treated with 5-Aza (2 μ M). In human tissues, DNMT1, DNMT3A, and DNMT3B are the most common methyltransferases that play key roles in various biological functions. We then explored the mechanism underlying the regulation of promotor methylation of ADAMTS9 DNA. AGS and BGC-823 cell lines were transfected with shDNMT1, shDNMT3A, or shDNMT3B (**Supplementary Figure S5**). PCR and Western blot analysis results showed that the DNMT3A should be the main methyltransferase that regulate ADAMTS9 expression (**Figure 4D**). DNA methylation analysis through MassARRAY platform also confirmed that downregulated DNMT1 and DNMT3A expressions significantly increased the methylation level of ADAMTS9 gene in the BGC823 cell, especially for DNMT3A (**Figure 4E** and **Supplementary Figures S4B** and **S4C**).

RNF180 restores ADAMTS9 expression by promoting DNMT3A ubiquitination and degradation

Our previous studies reported RNF180 plays the tumor suppressive roles on patients with GC. In this study, the IHC results of TMAs showed a significant positive correlation between RNF180 and ADAMTS9 expression. (N=126, Pearson $r=0.454$, $P<0.001$, **Figure 5A** and **Supplementary Figure S6**). In addition, with the correlation analysis from the GEPIA database (<http://gepia.cancer-pku.cn/>), we found that the mRNA expression level of RNF180 might be positively correlated with that ADAMTS9 (Spearman $r=0.28$, $P=5e-09$, Pearson $r=0.18$, $P=0.00024$, **Figure 5B**) Therefore, we hypothesized that the RNF180 restores ADAMTS9 expression by decreasing ADAMTS9 methylation. **Figure 5C** shows the results of PCR and Western blot analysis, which indicated that RNF180 upregulated ADAMTS9 expression through the epigenetic pathway. We then performed the methylation analysis of ADAMTS9 in the BGC823 cells transfected with RNF180, and the significant downregulated methylation of ADAMTS9 DNA was detected (**Figure 5D** and **Supplementary Figure S4D**). These results confirmed our previous hypothesis.

Considering that RNF180 restores the expression of ADAMTS9 by decreasing the methylation of ADAMTS9 promotor and that the methylation of ADAMTS9 promotor is mainly regulated by DNMT3A, we hypothesized that RNF180 ubiquitinated DNMT3A, which promoted their degradation via proteasome pathway. The CHX pulse-chase assay was performed to examine the function of RNF180 on DNMT3A stability. We observed that RNF180 promoted the degradation of DNMT3A protein and reduced their half-life. (**Figure 5E**). AGS and BGC823 cells were then incubated with MG132 (10 μ M) to inhibit protein

degradation via proteasome pathway. **Figure 5F** shows that RNF180 promoted the accumulation of DNMT3A after treatment with MG132. Hence, we speculated that DNMT3A might be the substrate of RNF180. To explore the interaction between RNF180 and DNMT3A, we performed the co-immunoprecipitation assay. The reciprocal co-immunoprecipitation confirmed the interaction between DNMT3A and RNF180 (**Figure 5G**). Ubiquitination assay was also performed to validate that the ubiquitination level of DNMT3A was greatly promoted by RNF180 (**Figure 5H**). In conclusion, ADAMTS9 was restored by RNF180 via promoting DNMT3A ubiquitination and degradation.

Discussion:

LN metastasis is a crucial factor to predict the survival outcomes, and the great understanding of the LN metastasis benefits how clinicians treat patients with GC. According to previous studies, ADAMTS9 is a tumor suppressor that inhibits the proliferation of several types of malignant tumors, such as esophageal⁸, and breast cancers¹⁰, GC¹², and nasopharyngeal carcinoma⁹. However, the involvement of ADAMTS9 in LN metastasis and as the predictive factor in GC have been rarely reported. In this study, we provided experimental and clinical evidences to support the suppressive effect of ADAMTS9 on LN metastasis in GC. Our study demonstrated that ADAMTS9 inhibited migration and invasion in GC cells. Clinical data suggested that the low expression of ADAMTS9 was closely associated with advanced pN stage and poor survival outcomes, which was identified as an independent risk factor. ADAMTS9 might be a potential biomarker to predict the risk of LN metastasis and improve the understanding of LN metastasis mechanism in GC.

The hypermethylation of CpG islands in the gene promotor region of ADAMTS9, which was detected by the MassARRAY analysis, was closely associated with the absent or down-regulated ADAMTS9 expression. And ADAMTS9 expression was largely regulated by the promotor methylation. These findings were consistent with those obtained in previous study¹². Silencing or promoting some tumor-related genes through hypermethylation or hypomethylation plays a crucial role in the occurrence and development of various cancer¹⁷. Thus, the potent molecular mechanism of the promotor methylation of ADAMTS9 must be investigated. In this study, ADAMTS9 expression was mostly inhibited by DNMT3A by enhancing the promotor methylation. DNMT1, DNMT3A, and DNMT3B are the three catalytic active DNMTs in mammals, which participate in a diverse range of biological processes¹⁸. DNMT3A and DNMT3B are responsible for the maintenance of DNA methylation through de novo methylation activity in the early stage of embryo or during cell differentiation, whereas DNMT1 is mostly responsible for the maintenance of DNA methylation during replication¹⁹. The disorder in the expression of DNMTs can elicit the hypo- or hyper-methylation of several tumor-related genes through epigenetic changes²⁰⁻²². Through the online GEPIA database and IHC staining in this study, we found a significant positive correlation between the expression of RNF180 and ADAMTS9. According to our previous studies, RNF180, which is an E3 ubiquitin ligase, is a suppressor gene that inhibits LN metastasis¹⁴. RNF180 belongs to the ubiquitin-proteasome system that plays an important role in several oncogenesis and tumor progression processes²³, whereas the substrate of RNF180 remains unclear. In present study, we uncovered that RNF180 could reduce the stability of

DNMT3A through the ubiquitination process, and that DNMT3A was identified as the substrate of RNF180. In such a process, RNF180, as a tumor suppressor, could restore some tumor-related genes, including ADAMTS9, and played a crucial role in impairing the lymphatic involvement of GC cells. In conclusion, ADAMTS9 was restored by RNF180-mediated ubiquitination and degradation of DNMT3A.

We further investigated the effect of ADAMTS9 on GC metastasis and its downstream molecular pathway. ADAMTS9 inhibited GC metastasis, mostly by regulating chemokine signaling pathway and cytokine–cytokine receptor interaction pathway, which were included in the top 20 KEGG enrichment pathways (**SupplementaryFigure S2**). Infection and chronic inflammation can promote tumor development in a tumor microenvironment. This phenomenon has become the hallmark of cancer, recently^{24,25}. The recruited stromal or inflammatory cells by tumor cells or by “educated” non-tumor cells through direct interaction or indirect signals (several cytokines and chemokines) constitute the tumor microenvironment²⁶. Chemokines is an important component of the tumor microenvironment and plays an important role in inflammation and also in cancer development²⁷. In this study, we demonstrated that ADAMTS9 inhibited LN metastasis in GC, through CCL5- and CXCL11-dependent pathways. First, CCL5/CCR5 axis is closely correlated with tumor metastasis^{28,29}. The high CCL5 or CCR5 expression in patients with GC were associated with a poor survival rate³⁰ and increased metastasis risk³¹. CCL5 could activate the $\alpha\beta3$ integrin through PI3K/Akt pathway, causing the upregulation of IKK alpha/beta and NF- κ B³², which eventually induced the secretion of MMP-9³³ or upregulated the secretion of both MMP-9 and MMP-2³⁴. CCL5 contributed to tumor cell metastasis by degrading the extracellular matrix. In addition, W Du et al. offered the indirect evidence that ADAMTS9 plays a tumor-suppressive effect through Akt pathway¹², which is mostly consistent with the downstream pathway of CCL5. The CCL5/CCR5 axis was the important intermediate element of ADAMTS9’s inhibition of the GC cell invasion and metastasis. Second, CXCL11 can increase the metastatic behavior of cancer cells in colorectal³⁵, ovarian³⁶, and prostate cancers³⁷. The mechanism of CXCL11 in promoting metastasis was based on the chemokine receptors CXCR3 and CXCR7³⁸. The mutual interaction of CXCR3 system and CXCR7 system formed a complex functional network³⁹. Even though CXCR3 and CXCR7 systems both regulate tumor growth and metastasis in various types of cancer⁴⁰, the explicit mechanism of CXCL11 currently remains unclear and must be further investigated. Nevertheless, CXCL11-CXCR3/CXCR7 axis can clearly contribute to tumor cell migration and invasion.

Conclusions:

In conclusion, the low ADAMTS9 expression was closely associated with advanced pN stage and poor survival outcome. Low ADAMTS9 expression might be a biomarker to predict the metastatic condition in patients with GC. ADAMTS9 expression was restored by RNF180 via promoting DNMT3A ubiquitination and degradation. ADAMTS9 inhibited GC cell metastasis by inactivating CCL5- and CXCL11-dependent pathways.

Limitations:

This study contains several potential limitations. First, the TMAs used in this study enrolled the GC tissues and adjacent non-tumor tissues between August 2004 and December 2007. Although TMAs were stored properly in -4 °C, some specimens were excluded, which might have caused evaluation bias. Second, the potential pathways of CCL5 and CXCL11 in various types of cancer have been extensively reported. In this study, we did not validate the downstream molecular mechanisms of CCL5 and CXCL11.

List Of Abbreviations:

ADAMTS9, a disintegrin-like and metalloprotease with thrombospondin type 1 motif 9; GC, gastric cancer; LN, lymph node; CCL5, C–C motif chemokine ligand 5; CXCL11, C–X–C motif chemokine ligand 11; DNMT, DNA-methyltransferase; RNF, Ring finger protein; TMA, tissue microarray; IHC, immunohistochemistry; CHX, cycloheximide; TCGA, The Cancer Genome Atlas; OS, overall survival; HR, hazard ratios; 95% CI, 95% confidence interval; DEG, differentially expressed genes.

Declarations:

Ethics approval and consent to participate

The study protocol and permission for the use of the clinical data and human tissue were given by the Institutional Research Ethics Committee of Tianjin Medical University Cancer Institute and Hospital (Tianjin, China).

Consent for publication

Not applicable.

Availability of data and materials

The datasets used and/or analysed during the current study are available from the corresponding author on reasonable request.

Competing interests

The authors declare that they have no competing interests.

Funding

This study was supported in part by grants from National Key Research and Development Program “precision medicine research” (2017YFC0908304), the Programs of National Natural Science Foundation of China (NO. 81572372), , National Key Research and Development Program “major chronic non-

infectious disease research” (2016YFC1303202), and the Natural Science Foundation of China (NO.81602153).

Authors' contributions

Jingyu Deng, Gang Ma, and Han Liang designed the experiments;

Weilin Sun, Gang Ma, Li Zhang, Pengliang Wang and Fenglin Cai conducted the experiments;

Weilin Sun, Huifang Liu, Nannan Zhang and Zizhen Wu Analyzed the data and prepared the figures;

Weilin Sun, Yinping Dong, Liqiao Chen and Zhenzhen Zhao wrote the manuscript;

Wei-lin Sun, Jing-yu Deng and Gang Ma equally contributed to the work.

The manuscript got the writing assistance from EssaySta (<https://essaystar.com/>) website.

Acknowledgements

The manuscript got the writing assistance from EssayStar(<https://essaystar.com/>) website.

References:

1. Bray F, Ferlay J, Soerjomataram I, et al. Global cancer statistics 2018: GLOBOCAN estimates of incidence and mortality worldwide for 36 cancers in 185 countries. *CA: a cancer journal for clinicians* 2018;68(6):394-424. doi: 10.3322/caac.21492
2. Karimi P, Islami F, Anandasabapathy S, et al. Gastric cancer: descriptive epidemiology, risk factors, screening, and prevention. *Cancer epidemiology, biomarkers & prevention : a publication of the American Association for Cancer Research, cosponsored by the American Society of Preventive Oncology* 2014;23(5):700-13. doi: 10.1158/1055-9965.EPI-13-1057
3. Clark ME, Kelner GS, Turbeville LA, et al. ADAMTS9, a novel member of the ADAM-TS/ metalloproteinase gene family. *Genomics* 2000;67(3):343-50. doi: 10.1006/geno.2000.6246
4. Ozler S, Isci Bostanci E, Oztas E, et al. The role of ADAMTS4 and ADAMTS9 in cardiovascular disease in premature ovarian insufficiency and idiopathic hypogonadotropic hypogonadism. *Journal of endocrinological investigation* 2018;41(12):1477-83. doi: 10.1007/s40618-018-0948-3
5. Kumagishi K, Nishida K, Yamaai T, et al. A disintegrin and metalloproteinase with thrombospondin motifs 9 (ADAMTS9) expression by chondrocytes during endochondral ossification. *Archives of histology and cytology* 2009;72(3):175-85. doi: 10.1679/aohc.72.175
6. Lo PH, Lung HL, Cheung AK, et al. Extracellular protease ADAMTS9 suppresses esophageal and nasopharyngeal carcinoma tumor formation by inhibiting angiogenesis. *Cancer research* 2010;70(13):5567-76. doi: 10.1158/0008-5472.CAN-09-4510

7. Koo BH, Coe DM, Dixon LJ, et al. ADAMTS9 is a cell-autonomously acting, anti-angiogenic metalloprotease expressed by microvascular endothelial cells. *The American journal of pathology* 2010;176(3):1494-504. doi: 10.2353/ajpath.2010.090655
8. Lo PH, Leung AC, Kwok CY, et al. Identification of a tumor suppressive critical region mapping to 3p14.2 in esophageal squamous cell carcinoma and studies of a candidate tumor suppressor gene, ADAMTS9. *Oncogene* 2007;26(1):148-57. doi: 10.1038/sj.onc.1209767
9. Lung HL, Lo PHY, Xie D, et al. Characterization of a novel epigenetically-silenced, growth-suppressive gene, ADAMTS9, and its association with lymph node metastases in nasopharyngeal carcinoma. *International journal of cancer* 2008;123(2):401-08. doi: 10.1002/ijc.23528
10. Shao B, Feng Y, Zhang H, et al. The 3p14.2 tumour suppressor ADAMTS9 is inactivated by promoter CpG methylation and inhibits tumour cell growth in breast cancer. *Journal of cellular and molecular medicine* 2018;22(2):1257-71. doi: 10.1111/jcmm.13404
11. Chen L, Tang J, Feng Y, et al. ADAMTS9 is Silenced by Epigenetic Disruption in Colorectal Cancer and Inhibits Cell Growth and Metastasis by Regulating Akt/p53 Signaling. *Cellular physiology and biochemistry : international journal of experimental cellular physiology, biochemistry, and pharmacology* 2017;44(4):1370-80. doi: 10.1159/000485534
12. Du W, Wang S, Zhou Q, et al. ADAMTS9 is a functional tumor suppressor through inhibiting AKT/mTOR pathway and associated with poor survival in gastric cancer. *Oncogene* 2013;32(28):3319-28. doi: 10.1038/onc.2012.359
13. Urnov FD. Methylation and the genome: the power of a small amendment. *The Journal of nutrition* 2002;132(8 Suppl):2450S-56S. doi: 10.1093/jn/132.8.2450S
14. Deng J, Liang H, Zhang R, et al. Clinical and experimental role of ring finger protein 180 on lymph node metastasis and survival in gastric cancer. *The British journal of surgery* 2016;103(4):407-16. doi: 10.1002/bjs.10066
15. Popovic D, Vucic D, Dikic I. Ubiquitination in disease pathogenesis and treatment. *Nature medicine* 2014;20(11):1242-53. doi: 10.1038/nm.3739
16. Kanehisa M, Araki M, Goto S, et al. KEGG for linking genomes to life and the environment. *Nucleic acids research* 2008;36(Database issue):D480-4. doi: 10.1093/nar/gkm882
17. Kulis M, Esteller M. DNA methylation and cancer. *Advances in genetics* 2010;70:27-56. doi: 10.1016/B978-0-12-380866-0.60002-2
18. Morgan AE, Davies TJ, Mc Auley MT. The role of DNA methylation in ageing and cancer. *The Proceedings of the Nutrition Society* 2018;77(4):412-22. doi: 10.1017/S0029665118000150
19. Fattahi S, Golpour M, Amjadi-Moheb F, et al. DNA methyltransferases and gastric cancer: insight into targeted therapy. *Epigenomics* 2018;10(11):1477-97. doi: 10.2217/epi-2018-0096
20. Gao Q, Steine EJ, Barrasa MI, et al. Deletion of the de novo DNA methyltransferase Dnmt3a promotes lung tumor progression. *Proceedings of the National Academy of Sciences of the United States of America* 2011;108(44):18061-6. doi: 10.1073/pnas.1114946108

21. Fu HY, Shen JZ, Wu Y, et al. Arsenic trioxide inhibits DNA methyltransferase and restores expression of methylation-silenced CDKN2B/CDKN2A genes in human hematologic malignant cells. *Oncology reports* 2010;24(2):335-43. doi: 10.3892/or_00000864
22. Zheng Y, Huang Q, Ding Z, et al. Genome-wide DNA methylation analysis identifies candidate epigenetic markers and drivers of hepatocellular carcinoma. *Briefings in bioinformatics* 2018;19(1):101-08. doi: 10.1093/bib/bbw094
23. Cheung KF, Lam CN, Wu K, et al. Characterization of the gene structure, functional significance, and clinical application of RNF180, a novel gene in gastric cancer. *Cancer* 2012;118(4):947-59. doi: 10.1002/cncr.26189
24. Bottcher JP, Bonavita E, Chakravarty P, et al. NK Cells Stimulate Recruitment of cDC1 into the Tumor Microenvironment Promoting Cancer Immune Control. *Cell* 2018;172(5):1022-37 e14. doi: 10.1016/j.cell.2018.01.004
25. Halama N, Zoernig I, Berthel A, et al. Tumoral Immune Cell Exploitation in Colorectal Cancer Metastases Can Be Targeted Effectively by Anti-CCR5 Therapy in Cancer Patients. *Cancer cell* 2016;29(4):587-601. doi: 10.1016/j.ccell.2016.03.005
26. Yang L, Lin PC. Mechanisms that drive inflammatory tumor microenvironment, tumor heterogeneity, and metastatic progression. *Seminars in cancer biology* 2017;47:185-95. doi: 10.1016/j.semcancer.2017.08.001
27. Chow MT, Luster AD. Chemokines in cancer. *Cancer immunology research* 2014;2(12):1125-31. doi: 10.1158/2326-6066.CIR-14-0160
28. Zhang Q, Qin J, Zhong L, et al. CCL5-Mediated Th2 Immune Polarization Promotes Metastasis in Luminal Breast Cancer. *Cancer research* 2015;75(20):4312-21. doi: 10.1158/0008-5472.CAN-14-3590
29. Aldinucci D, Casagrande N. Inhibition of the CCL5/CCR5 Axis against the Progression of Gastric Cancer. *International journal of molecular sciences* 2018;19(5) doi: 10.3390/ijms19051477
30. Sugasawa H, Ichikura T, Tsujimoto H, et al. Prognostic significance of expression of CCL5/RANTES receptors in patients with gastric cancer. *Journal of surgical oncology* 2008;97(5):445-50. doi: 10.1002/jso.20984
31. Wang T, Wei Y, Tian L, et al. C-C motif chemokine ligand 5 (CCL5) levels in gastric cancer patient sera predict occult peritoneal metastasis and a poorer prognosis. *International journal of surgery* 2016;32:136-42. doi: 10.1016/j.ijsu.2016.07.008
32. Huang CY, Fong YC, Lee CY, et al. CCL5 increases lung cancer migration via PI3K, Akt and NF-kappaB pathways. *Biochemical pharmacology* 2009;77(5):794-803. doi: 10.1016/j.bcp.2008.11.014
33. Long H, Xie R, Xiang T, et al. Autocrine CCL5 signaling promotes invasion and migration of CD133+ ovarian cancer stem-like cells via NF-kappaB-mediated MMP-9 upregulation. *Stem cells* 2012;30(10):2309-19. doi: 10.1002/stem.1194
34. Kato T, Fujita Y, Nakane K, et al. CCR1/CCL5 interaction promotes invasion of taxane-resistant PC3 prostate cancer cells by increasing secretion of MMPs 2/9 and by activating ERK and Rac signaling. *Cytokine* 2013;64(1):251-7. doi: 10.1016/j.cyto.2013.06.313

35. Gao YJ, Liu L, Li S, et al. Down-regulation of CXCL11 inhibits colorectal cancer cell growth and epithelial-mesenchymal transition. *OncoTargets and therapy* 2018;11:7333-43. doi: 10.2147/OTT.S167872
36. Koo YJ, Kim TJ, Min KJ, et al. CXCL11 mediates TWIST1-induced angiogenesis in epithelial ovarian cancer. *Tumour biology : the journal of the International Society for Oncodevelopmental Biology and Medicine* 2017;39(5):1010428317706226. doi: 10.1177/1010428317706226
37. Wang Y, Xu H, Si L, et al. MiR-206 inhibits proliferation and migration of prostate cancer cells by targeting CXCL11. *The Prostate* 2018;78(7):479-90. doi: 10.1002/pros.23468
38. Puchert M, Obst J, Koch C, et al. CXCL11 promotes tumor progression by the biased use of the chemokine receptors CXCR3 and CXCR7. *Cytokine* 2020;125:154809. doi: 10.1016/j.cyto.2019.154809
39. Singh AK, Arya RK, Trivedi AK, et al. Chemokine receptor trio: CXCR3, CXCR4 and CXCR7 crosstalk via CXCL11 and CXCL12. *Cytokine & growth factor reviews* 2013;24(1):41-9. doi: 10.1016/j.cytogfr.2012.08.007
40. Freitas C, Desnoyer A, Meuris F, et al. The relevance of the chemokine receptor ACKR3/CXCR7 on CXCL12-mediated effects in cancers with a focus on virus-related cancers. *Cytokine & growth factor reviews* 2014;25(3):307-16. doi: 10.1016/j.cytogfr.2014.04.006

Figures

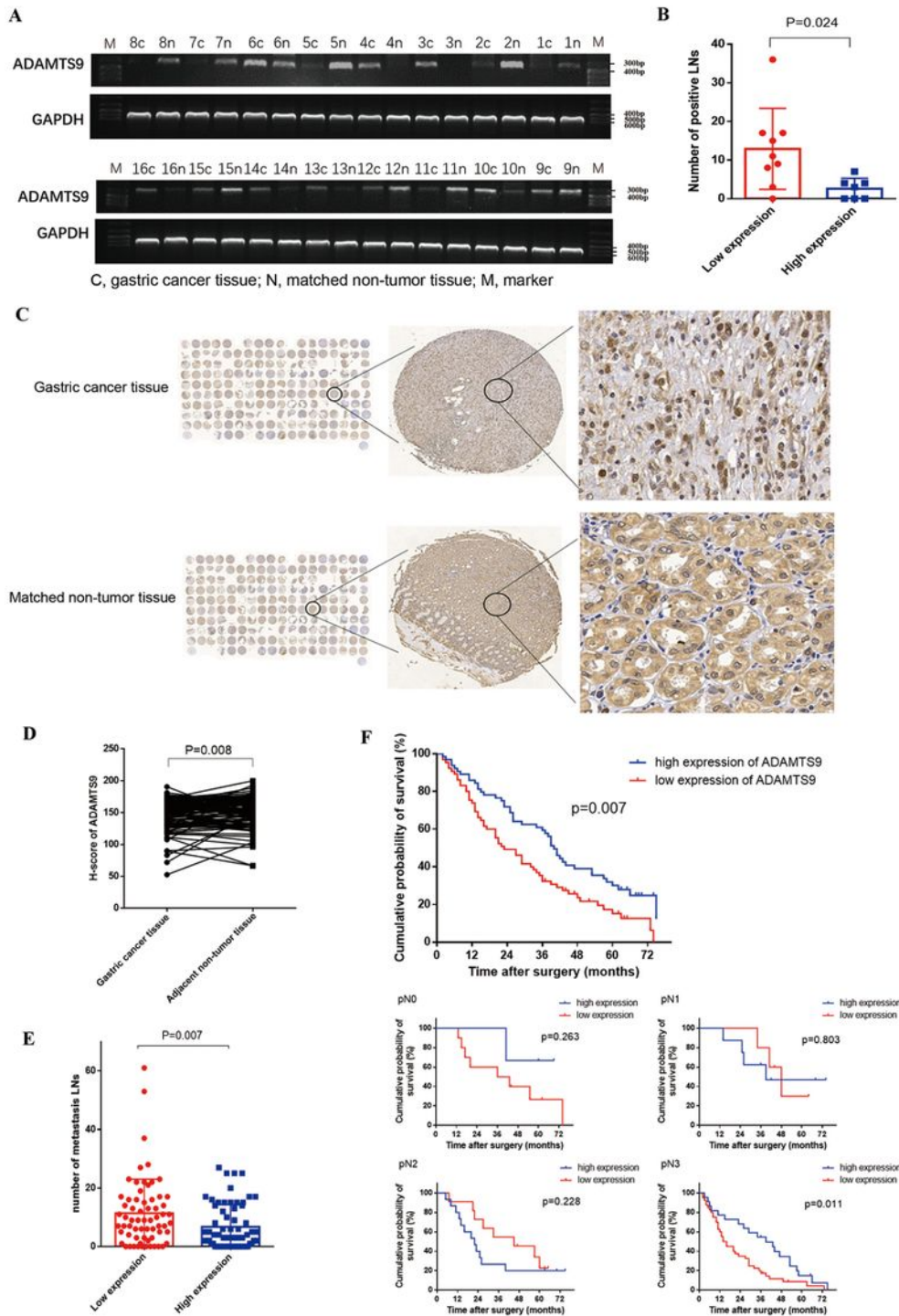


Figure 1 Low expression of ADAMTS9 in GC is associated with more metastatic lymph nodes and poorer survival outcomes.

Figure 1

Low expression of ADAMTS9 in GC is associated with more metastatic lymph nodes and poorer survival outcomes. (A) mRNA expression levels of ADAMTS9 in GC tissues and matched non-tumor tissues. (B) Association between ADAMTS9 mRNA expression and metastatic lymph nodes. (C) IHC of ADAMTS9 in GC tissues and matched adjacent non-tumor tissues. (D) Low expression of ADAMTS9 protein in GC

tissues. (E) Association between the expression of ADAMTS9 protein and metastatic lymph nodes. (F) Kaplan Meier survival analysis in 129 GC patients and stratification by pN stage.

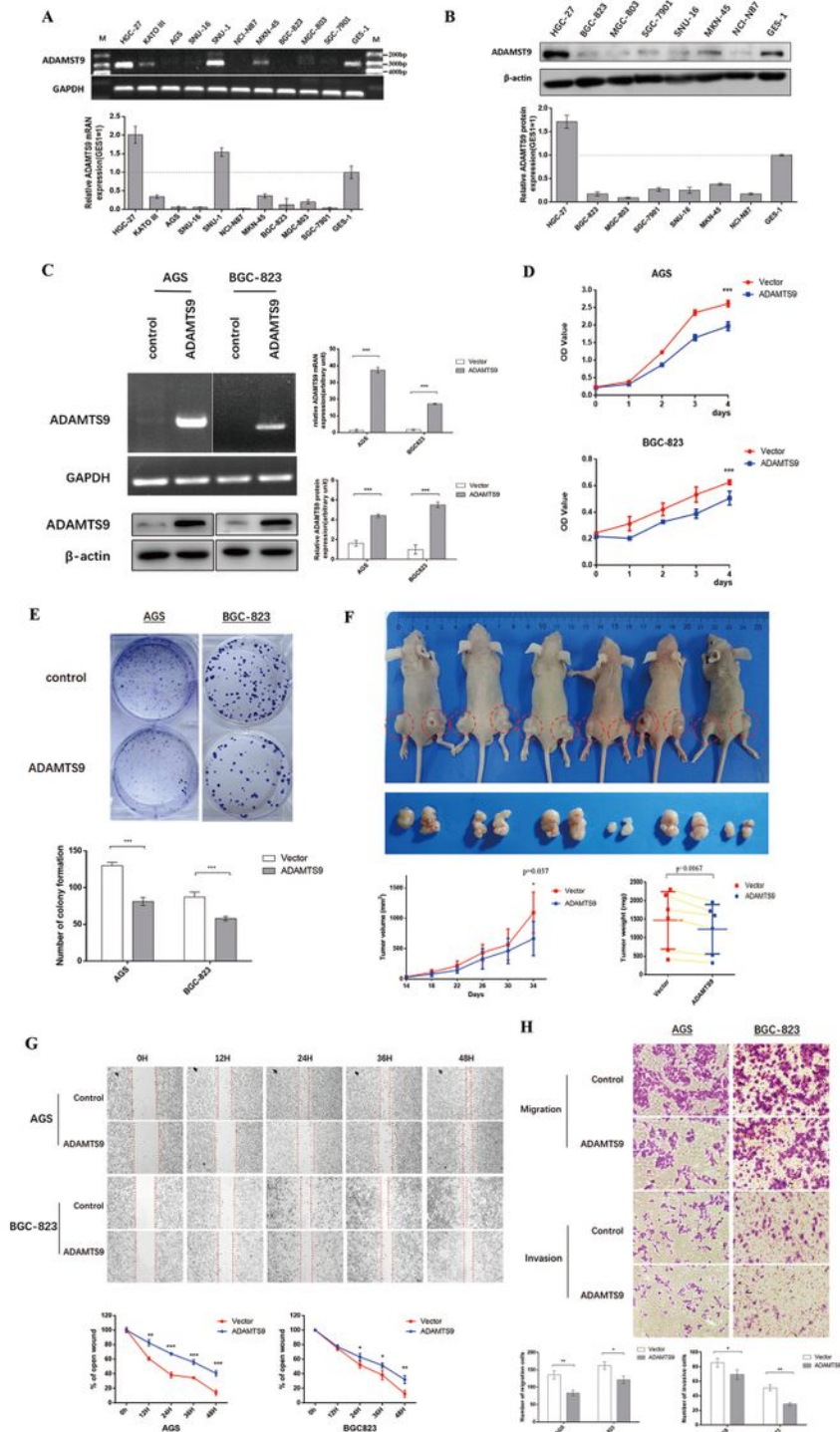


Figure 2 The ADAMTS9 expression in GC cell lines and biology function of ADAMTS9 in GC

Figure 2

The ADAMTS9 expression in GC cell lines and biology function of ADAMTS9 in GC. (A) mRNA expression levels of ADMATS9 in ten GC cell lines and normal human gastric epithelial cell line (GES-1). (B) Western blotting of protein level from seven GC cell lines and normal human gastric epithelial cell line (GES-1) for

ADAMTS9 expression. (C) mRNA and protein expression levels of ADAMTS9 in AGS and BGC-823 cells transfected with ADAMTS9 overexpression plasmid and empty plasmid. (D) ADAMTS9 inhibits the cell growth in AGS and BGC-823 cells. (E) ADAMTS9 suppresses the colony formation in AGS and BGC-823 cells. (F) ADAMTS9 inhibited growth of tumors in vivo. Tumor growth curves and tumor weight shows the suppressive effect of ADAMTS9 in vivo. (G) ADAMTS9 impairs motile capacity in AGS and BGC-823 cells detected by wound healing assay; (H) and by transwell assay.

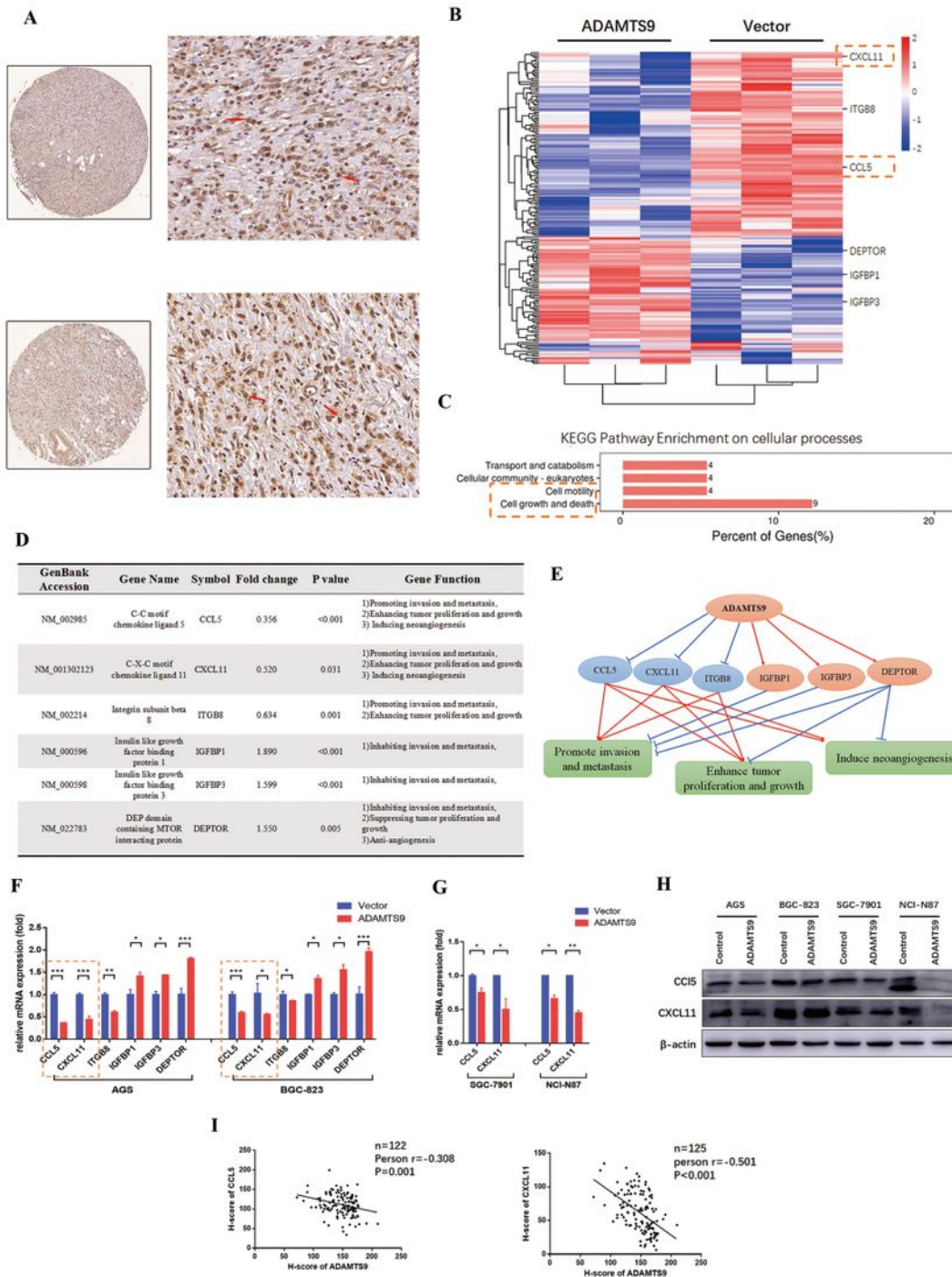


Figure 3 ADAMTS9 downregulates the expression of CCL5 and CXCL11.

ADAMTS9 downregulates the expression of CCL5 and CXCL11. (A) ADAMTS9 is partly located in the nucleus of the gastric tissue cells. (B) The heatmap was generated from mRNA sequencing analysis of ADAMTS9-overexpressing BGC-823 cells and control cells transfected with empty plasmid. (C) KEGG analysis of DEGs on cellular processes. (D) The foldchange and P-value of downstream potent molecular. (E) Downstream potent molecular event for impairing viability, proliferation and motile capacity. (F) The downstream DEGs were confirmed by the qPCR in AGS and BGC-823 cells. (G) ADAMTS9 also inhibits transcription of CCL5 and CXCL11 in other two gastric cell lines, SGC-7901 and NCI-N87 cells, detected by qPCR; (H) ADAMTS9 downregulates the protein expression of CCL5 and CXCL11 in four gastric cell lines, detected by western blotting method. (I) IHC of TMAs shows a significant negative association between ADAMTS9 and CCL5, and between ADAMTS9 and CXCL11.

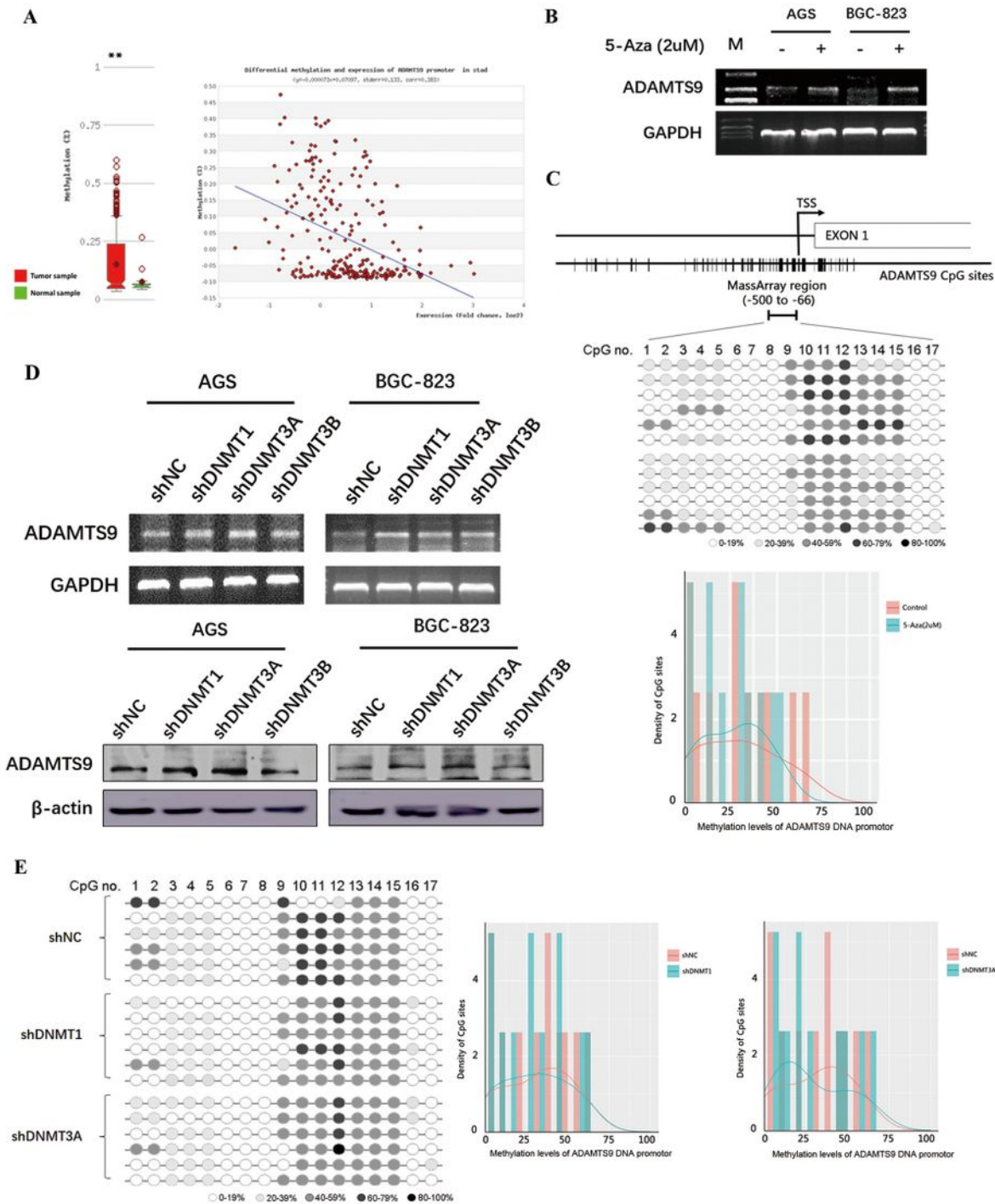


Figure 4 Hypermethylated ADAMTS9 in gastric cancer is mainly associated with DNMT3A

Figure 4

Hypermethylated ADAMTS9 in gastric cancer is mainly associated with DNMT3A. (A) ADAMTS9 DNA promoter is hypermethylated in the gastric cancer, according to the MethHC database. (B) The ADAMTS9 expression in AGS and BGC-823 cells after pharmacological reversal of DNA methylation by 5-Aza was examined by reverse transcriptase PCR. (C) The MassARRAY analysis spans the promoter region from -500 to -66, including 17 CpG islands. The methylation levels of ADAMTS9 DNA promoter after 5-Aza

incubation were showed. (D) The expression of ADAMTS9 in AGS and BGC-823 cells was examined by reverse transcriptase PCR and western blotting method, after transfection with shDNMT1, shDNMT3A, shDNMT3B or empty plasmid. (E) The methylation levels of ADAMTS9 DNA promoter after transfection were detected by the MassARRAY analysis.

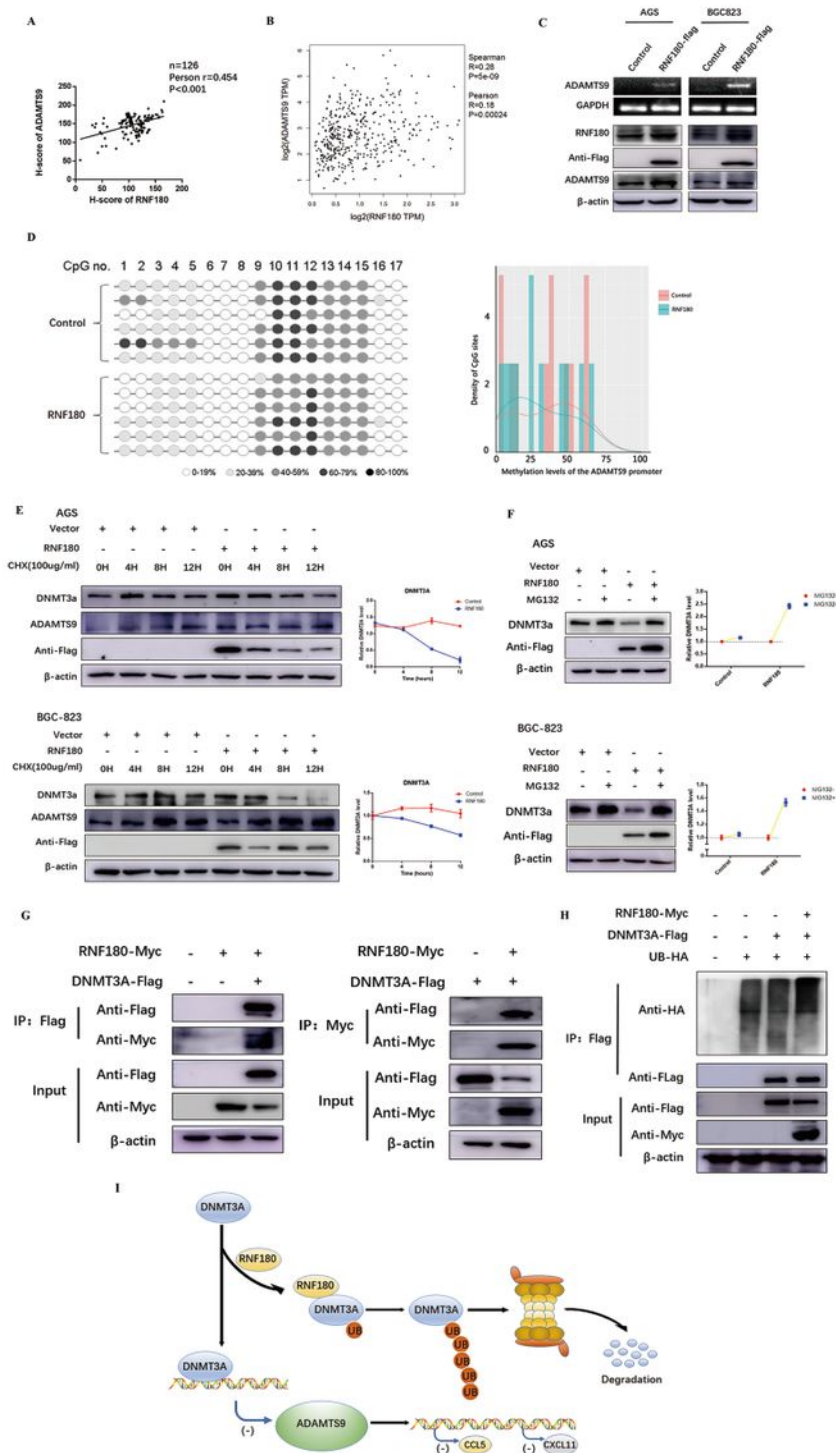


Figure 5 . RNF180 restored ADAMTS9 expression by promoting DNMT3A ubiquitination and degradation.

Figure 5

RNF180 restored ADAMTS9 expression by promoting DNMT3A ubiquitination and degradation. (A) The expression of RNF180 has a significant positive correlation with the expression of ADAMTS9, according to IHC of TMAs; (B) and the online DEPIA database. (C) The expression of ADAMTS9 was examined by PCR and western blotting method, after transfection with RNF180-overexpression plasmid. (D) The methylation levels of ADAMTS9 DNA promoter after transfection were examined by the MassARRAY analysis. (E) AGS and BGC-823 cells were transfected by RNF180-Flag plasmid or control vector. After 48 h, cells were treated with 100 mg/ml CHX at the indicated time point. The DNMT3A, ADAMTS9 and RNF180-Flag proteins were measured through western blotting method. (F) AGS and BGC-823 cells were transfected by RNF180-Flag plasmid or control vector. After 48 h, cells were incubated with 10 uM MG132 for 24h. The DNMT3A and RNF180-Flag proteins were measured through western blotting method. (G) RNF180-Myc plasmid or control vector was co-transfected transiently with the DNMT3A-Flag plasmid or control vector into HEK293T cells. After transfection 36h, HEK293T cells were treated with 10 uM MG132 for 12h. Then, Co-immunoprecipitation assay was performed to pull down DNMT3A-Flag and RNF180-Myc proteins and the immunoprecipitated proteins were measured through western blotting method. (H) UB-HA and DNMT3A-Flag plasmids were co-transfected with RNF180-Myc plasmid into HEK293T cells. After 36 h, HEK293T cells were treated with 10 uM MG132 for 12h. DNMT3A-Flag protein was immunoprecipitated and measured by western blotting method. The poly-ubiquitination level of DNMT3A was detected by anti-HA antibody.

Supplementary Files

This is a list of supplementary files associated with this preprint. Click to download.

- [Supplementarydataset.docx](#)
- [SupplementaryTable.docx](#)
- [Sfigure2.jpg](#)
- [Sfigure5.jpg](#)
- [Sfigure6.jpg](#)
- [Sfigure3.jpg](#)
- [Sfigure1.jpg](#)
- [Sfigure4.jpg](#)